J. Fluid Mech. (1972). *vol.* 51, *part* 1, *pp.* 69–95
Printed in Great Britain

On the noise of a nearly ideally expanded supersonic jet

By CHRISTOPHER K. W. TAM†

Department of Aeronautics and Astronautics,
Massachusetts Institute of Technology

(Received 1 June 1971)

A noise generation mechanism for a nearly ideally expanded supersonic jet is proposed. It is suggested that the dominant part of the noise of a supersonic jet is generated at two rather localized regions of the jet. These regions are located at distances quite far downstream of the nozzle exit. Large-scale instabilities of the jet flow are believed to be responsible for transferring the kinetic energy of the jet into noise radiation. An analysis based on a simple mathematical model reveals that two large-scale unstable waves are preferentially amplified in a supersonic jet. The rapid growth of these waves causes the oscillations of the jet to penetrate the mixing layer at two locations and to interact strongly with the ambient fluid there. This gives rise to intense noise radiation. Theoretical results based on the proposed noise generation mechanism are found to compare favourably with experimental measurements. A simple scaling formula is also derived.

1. Introduction

Lighthill's aerodynamic noise theory (1952, 1954) and subsequent extensions developed by others, for example, Ribner (1964) and references thereof on subsonic jets, have provided a good deal of understanding on jet noise generation over the years. Lighthill's original idea was that turbulence in the highly sheared regions close to the nozzle exit of a subsonic jet is the dominant noise generation mechanism. With this physical insight he was able to deduce by reformulating the flow equations into an acoustic wave equation with source terms that the total power of noise radiated from a subsonic jet varies as the eighth power of the jet velocity. This simple scaling formula has since been confirmed experimentally (see Lighthill 1963) over a wide range of jet velocities. Unfortunately, as the jet velocity increases above the speed of sound the U^8 law becomes inapplicable, indicating that some other noise generated mechanisms may become effective at high jet velocity. To account for the discrepancy Ffowcs Williams (1963) extended Lighthill's theory to high-speed jets. The mathematical theory developed by him revealed that for a high-speed jet the radiated noise was in the form of eddy Mach waves. Earlier, Phillips (1960), on starting from a different reformulation of the flow equations, had proposed the eddy Mach wave concept when considering the noise produced from a supersonic free shear layer. A precise physical picture of eddy Mach wave radiation has never been given by Phillips or Ffowcs Williams,

† Present address: Department of Mathematics, Florida State University.

yet many authors have associated the Mach waves with the analogy of supersonic flow over a wavy wall, e.g. Ribner (1969). Acoustic waves from a supersonic jet which have the general features of Mach waves have been identified experimentally, but so far there is no concrete evidence that they are indeed generated by turbulent eddies. Moreover, as far as the dominant part of supersonic jet noise is concerned, recent far and near field measurements (see Potter 1968; Ollerhead 1967; Yu & Dosanjh 1971) are found to be totally inconsistent with the idea that they are produced by eddy Mach waves. There is a strong indication that some other noise generation mechanism is responsible for the noise (dominant part) of a supersonic jet.

In the flow field of a supersonic jet the most highly sheared region is the mixing layer on the outer part of the jet immediately downstream of the nozzle exit. Hence this would be the place most favourable for the production of turbulent eddies. Also the eddy convection velocity will be higher here (a favourable condition for the emission of eddy Mach waves) than in other parts of the jet. If eddy Mach waves are the dominant sources of noise it is natural to expect most of the noise to come from this region. That is to say, if eddy Mach waves were the dominant noise generation mechanism, the dominant noise sources of a supersonic jet are likely to be located quite close to the nozzle exit.

In recent years a good deal of effort has been spent by various authors, for example, Ollerhead (1966), Lowson & Ollerhead (1968), Dosanjh & Yu (1968) in the search for eddy Mach waves experimentally using optical means. As yet, no concrete positive statement can be made. Shadowgraphs of supersonic jets taken by these authors and others and schlieren photographs taken by Eggers (1966), Jones (1971) and others show that immediately downstream of the nozzle exit certain waves can be observed which may be interpreted as Mach waves. Actually there are two distinct sets of waves which appear to have parallel wave fronts on shadowgraphs and schlieren pictures. Shadowgraphs tend to show the high-frequency waves more eminently. These waves are emitted from the shear layer very close to the nozzle exit not exceeding a few jet diameters in extent. They have been studied by the present author (Tam 1971) and have been shown to be the direct result of shear layer instability. The lower-frequency waves do not seem to appear very prominently in shadowgraphs (although they can still be identified in good quality shadowgraphic pictures) but can readily be seen in schlieren photographs. These waves originate from the edge of the core of the supersonic jet starting from the nozzle exit to as far as 8 to 10 jet diameters downstream depending on the Mach number of the jet. Even though these waves possess many salient features that are expected of eddy Mach waves such an interpretation is not without difficulties. First of all, if the angle between the parallel wave fronts and the jet axis is used to estimate the eddy convection velocity an unexpectedly high value of ~ 0.75 times the mean jet exit speed or higher is found whereas a value much closer to 0·5 is anticipated. Second, the wave fronts form almost parallel straight lines indicating that the eddies are convected at more or less a single speed. It is hard to conceive why only eddies moving at this particular velocity would radiate sound waves. Third, on the schlieren pictures the wave fronts are exceedingly ordered and coherent. To

produce such waves a turbulent eddy must start to radiate continuously immediately after it is formed near the nozzle exit until it has travelled to a distance of 8–10 jet diameters downstream. From boundary-layer and related works one would expect an eddy to become uncorrelated after it has travelled a distance of, say, six times its own size (or characteristic thickness of the boundary or mixing layer). Therefore, to be able to produce such an ordered and coherent wave pattern as is observed, the turbulent eddies must have an extraordinarily long lifetime.

Whether the observed waves are indeed Mach waves or not is irrelevant as far as the dominant part of the noise of a supersonic jet is concerned. Far and near field noise measurements by Yu & Dosanjh (1971), Potter (1968) and others show that the frequencies of these waves observed optically are very much higher than the dominant noise frequencies obtained by microphone measurements. In fact this high frequency noise does not even make any significant contribution to the total power of noise radiated. In addition, the location of dominant noise sources has been found not to be near the nozzle exit of a supersonic jet as would be

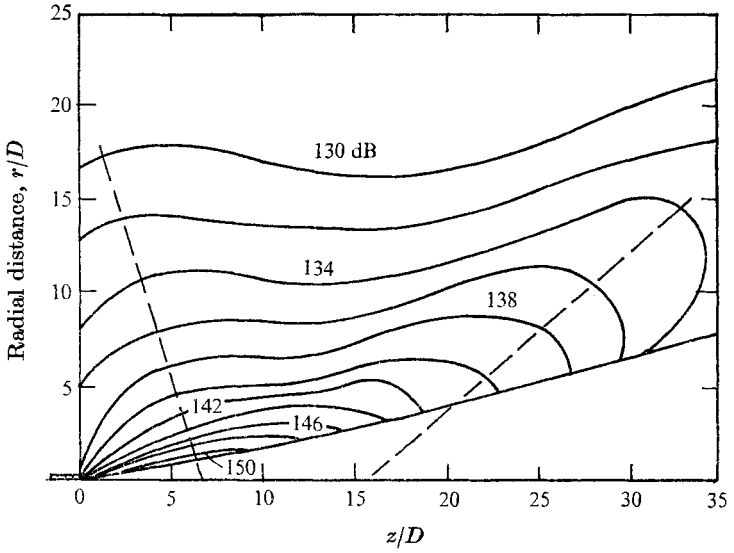

FIGURE 1. Contours of near field sound pressure level of a supersonic jet (M_j = 1·5), data from Yu & Dosanjh.

expected of Mach wave radiation but much farther downstream. Figure 1 shows the overall sound pressure contours of a nearly ideally expanded cold supersonic jet of Mach number 1·5 measured by Yu & Dosanjh (see also figure 8 of Mull & Erickson (1957)). If one extrapolates back from the far field noise contours (broken lines in figure 1) it is easy to see that there are two strong but localized noise sources both of which are located more than 6 jet diameters downstream. Also Mayes, Lanford & Hubbard (1959) have carried out some extensive noise measurements on rocket engines. Figure 2 shows contours of equal noise intensity of a small rocket measured by them. It suggests strongly that most of the noise is produced by a powerful localized noise source situated at about 20 exit diameters

downstream. Potter (1968) realized the disagreement between Mach wave theory and earlier noise measurements and carried out a series of experiments to locate the acoustic sources in a high-speed jet using a reverberation chamber. A Mach 2·5 shock-free cold nitrogen jet was employed in his study. His results agree with other experimental measurements and indicate a dominant noise source located at round 20 jet diameters downstream.

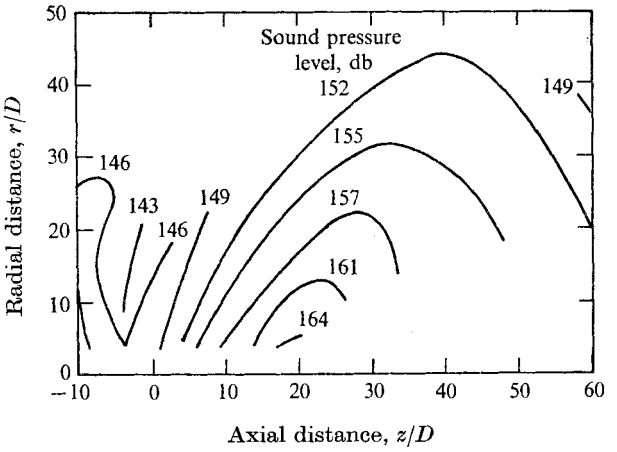

FIGURE 2. Contours of near field sound pressure level for a small rocket, data from Mayes, Lanford & Hubbard.

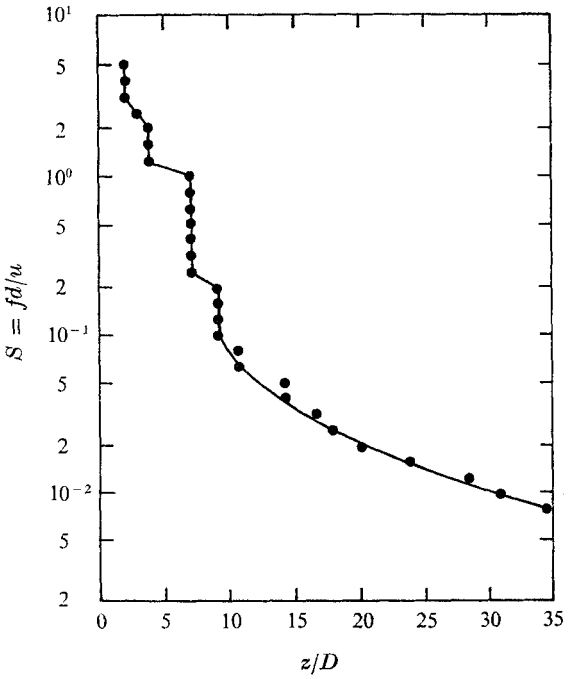

FIGURE 3. Location of apparent sources in ($\frac{1}{3}$ octave band) a supersonic jet (M_j = 1·5), data from Yu & Dosanjh.

The disagreement between Mach wave theory and experiment is perhaps far too great for possible reconciliation. Now let us examine existing supersonic jet noise data in some detail and try to draw some general conclusions as to the distribution of noise sources and the shape of noise power spectrum with which any other proposed supersonic jet noise theory must be consistent. With regard to this we will limit our present effort and also all the subsequent considerations in this paper to jets which are operated at nearly shock-free conditions. This helps to

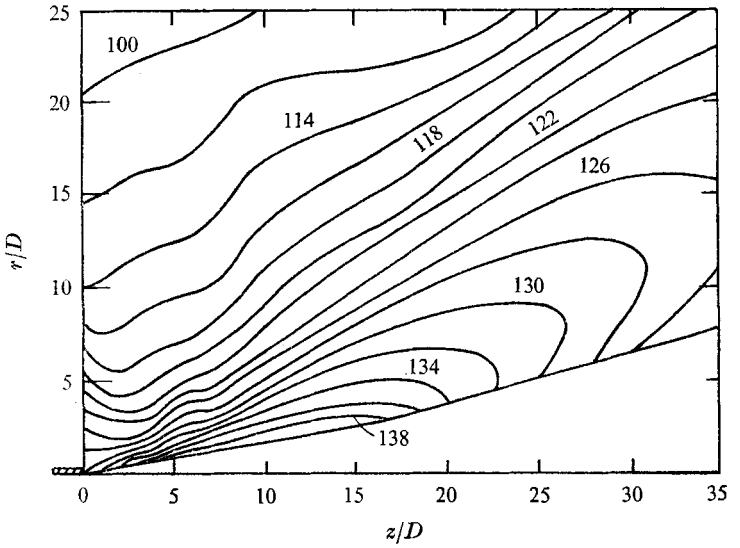

FIGURE 4. $\frac{1}{3}$ octave band sound pressure contours of a supersonic jet (M_j = 1·5). Centre frequency = 10 kHz, data from Yu & Dosanjh.

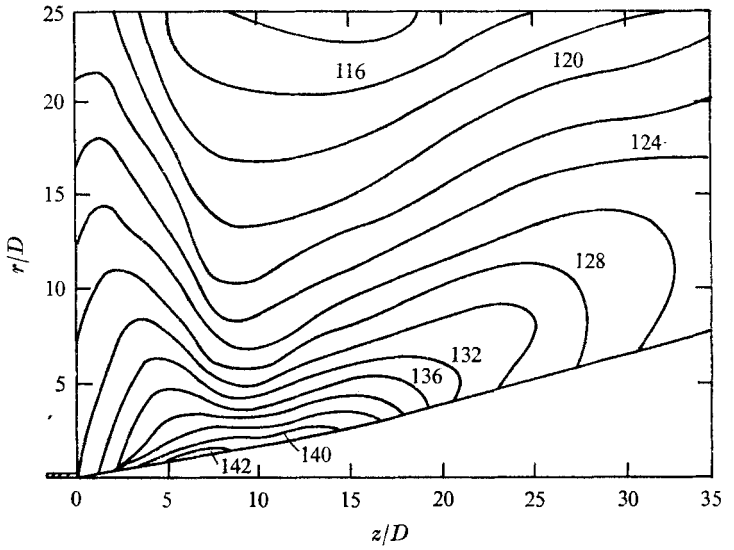

FIGURE 5. $\frac{1}{3}$ octave band sound pressure contours of a supersonic jet (M_j = 1·5). Centre frequency = 20 kHz, data from Yu & Dosanjh.

remove the great complication of shock generated noise that arises when strong shocks are present in the jet flow. It is evident that noise comes from a good part of the flow field of a supersonic jet even though some of this noise might not contribute in any significant way to the overall jet noise power. The general distribution of these apparent noise sources in terms of frequencies can be inferred approximately from near field noise measurements for supersonic jets. Figure 3 is a plot of the Strouhal number of these noise sources as a function of distance downstream of the nozzle exit given by Yu & Dosanjh (1971). This figure shows qualitatively that close to the nozzle the jet emits predominantly high frequency noise while most of the low frequency noise comes from parts of the jet much farther downstream. This general feature of frequency distribution is in good agreement

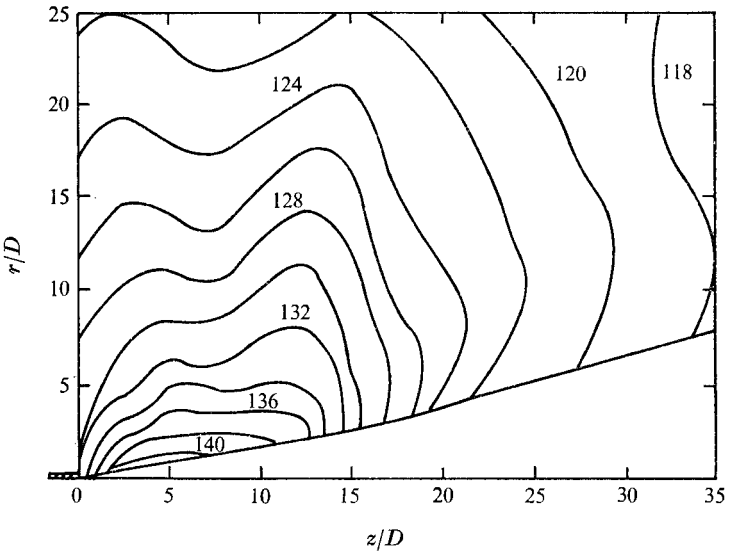

FIGURE 6. $\frac{1}{3}$ octave band sound pressure contours of a supersonic jet ($M_j = 1{\cdot}5$). Centre frequency = 50 kHz, data from Yu & Dosanjh.

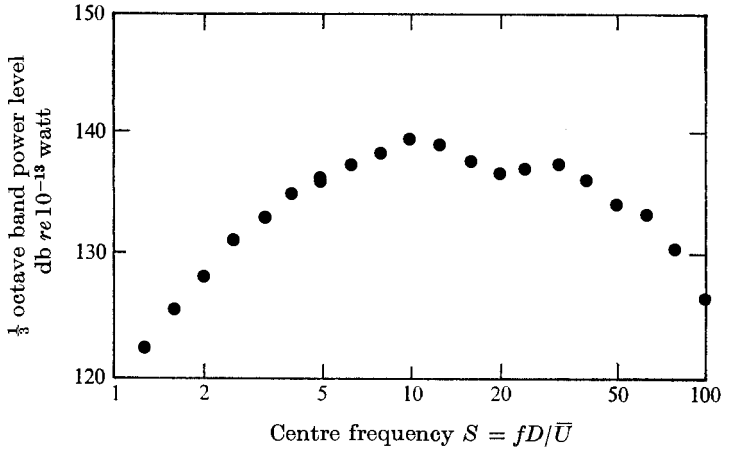

FIGURE 7. $\frac{1}{3}$ octave band power spectrum ($M_j = 2{\cdot}23$), data from Dosanjh & Yu, $\frac{1}{3}$ octave band power level db *re* 10^{-13} watt.

with the findings of Mull & Erickson (1957) using a much higher Mach number jet (pressure ratio equal to 30). Apart from this general frequency distribution pattern, near and far field noise measurements of various authors do indicate that a large fraction of the total noise power comes from one or two highly localized parts of the jet. The work of Yu & Dosanjh (1971) and Mull & Erickson (1957) suggests unambiguously that two such powerful sources exist, see figure 1. Figures 4, 5 and 6 are noise data taken by Yu & Dosanjh. A similar series of figures can also be found in the work of Mull & Erickson. In these figures $\frac{1}{3}$ octave band sound pressure contours at centre frequencies of 10, 20 and 50 kHz are displayed.

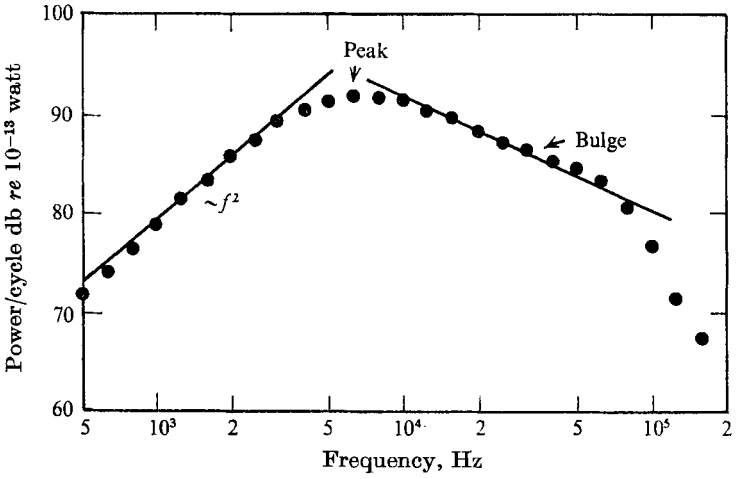

FIGURE 8. Power spectrum of a supersonic jet ($M_j = 1.5$), data from Yu & Dosanjh, power/cycle db *re* 10^{-13} watt.

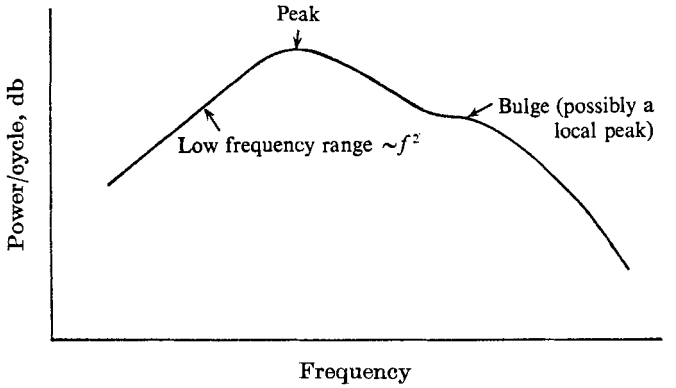

FIGURE 9. General features of the power spectrum of a shock-free supersonic jet.

These figures point out that of the two powerful noise sources the one closer to the nozzle radiates mostly high frequency noise and is much weaker in the total power of noise radiated. It is our belief that because of these disparities in noise source strength and frequencies many other experimenters failed to identify the localized high frequency noise source. Clues on the existence of two powerful

noise sources in an almost shock-free supersonic jet can also be found from the total noise power spectrum. Figure 7 is a $\frac{1}{3}$ octave band power spectrum of a slightly under-expanded supersonic jet obtained by Dosanjh & Yu (1968). Two distinct peaks are exhibited. They strongly imply that there are two strong noise sources which emit noise predominantly at two rather narrow bands of frequencies. Of course, the power spectrum (power per cycle) and not the $\frac{1}{3}$ octave band power spectrum is the proper physically meaningful entity. On converting to power per cycle the minor peak of figure 7 becomes less distinct. The data points are too far apart to tell whether a minor local peak still exists. In any case a definite bulge (see figure 9) in the power spectrum is unmistakably present. A similar bulge can also be noticed in figure 8 which is the power spectrum of the noise of the jet studied by Yu & Dosanjh. Figure 9 is a sketch of the noise power spectrum of an almost shock-free supersonic jet based on experimental measurements of various authors mentioned above. It shows that such a power spectrum is dominated by a peak with a small bulge or possibly a local peak at a higher frequency. In the low frequency range, the power spectral density p_f seems to follow a simple scaling formula of $p_f \propto f^2$. However, there is not enough experimental data available to establish the behaviour of the power spectral density above the frequency of the bulge.

In this paper a noise generation mechanism for a nearly ideally expanded supersonic jet based on the concept of large-scale instabilities of the jet flow is proposed. It will be shown that the results predicted by the present theory are consistent with experimental observations described above. In §2 a physical picture of the proposed noise generation mechanism is described. The necessary mathematical details concerning the present proposal are developed in §§3, 4 and 5. A theoretical formula for the frequency corresponding to the peak value of the power spectrum of the radiated noise from a supersonic jet is given in §6. Comparisons between some quantitative predictions of the present paper and existing available experimental data are made in §7. In §8 a simple scaling formula which is the natural consequences of the proposed mechanism is derived on physical grounds. The effect of jet temperature on the dominant frequencies of jet noise and the noise of underexpanded and overexpanded supersonic jets are briefly discussed in the final section of this paper.

2. A proposed mechanism

Unsteadiness in the flow field of a jet is, perhaps, one of the most effective ways by which noise can be generated. Unsteadiness can be caused in a variety of ways, by, for example, turbulent mixing at the jet boundary, turbulence convected out of the jet nozzle or it can also be generated by intrinsic hydrodynamic instabilities of the flow field. Theoretical investigations (Lessen, Fox & Zien 1965; Gill & Drazin 1965; Michalke 1965; Berman & Ffowcs Williams 1970; Tam 1971 and others) have shown that the flow of a jet is highly unstable. Near the nozzle exit the mixing layer is thin and a host of instabilities with relatively short wavelength can occur. This type of shear layer instabilities has wavelengths scaled according to the mixing-layer thickness. These short-wave instabilities

principally involve the jet fluid in the mixing layer and hence contain only a small fraction of the kinetic energy of the jet. They are rather mild and are not strong enough to disrupt the main jet flow. On the other hand, a supersonic jet is also subjected to large-scale long-wave instabilities with scale length equal to the diameter of the jet. When large-scale instability takes place all the fluid in the jet from inside the jet core to the mixing layer participates. Therefore these instabilities are rather violent as a sizeable fraction of the kinetic energy of the jet could be transformed into unsteady motion in their presence. Also they often lead to a rapid destruction of the jet itself.

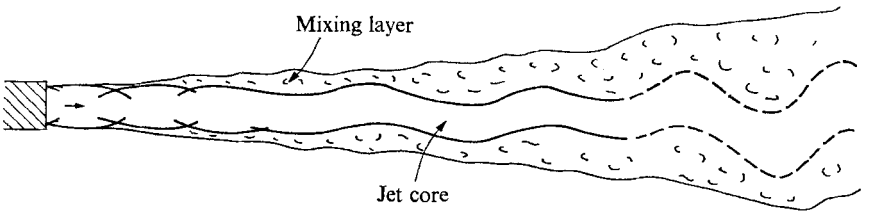

FIGURE 11. Sketch of large-scale spiral-mode instability of a nearly ideally expanded supersonic jet.

In this paper we proposed that most of the noise from a nearly ideally expanded supersonic jet is generated by the interaction of large-scale instabilities in the jet flow and the ambient fluid. For subsonic jets a similar idea related to large-scale puffs has been explored by Crow & Champagne (1970). The existence of large-scale instabilities in supersonic jets can easily be seen in shadowgraphs obtained by various authors, for example, Ollerhead (1967), Lowson & Ollerhead (1968), Potter (1968), even though the significance of these instabilities has not been noticed before. Figure 10 (plate 1) (see also sketch on figure 11) is a shadowgraph of a cold supersonic nitrogen jet of Mach number 2·53 taken at the M.I.T. Gas Turbine Laboratory. In this shadowgraph large-scale oscillations of the supersonic jet core can easily be seen. A systematic study of all available shadowgraphs suggests that these large-scale instabilities have a spiral-mode geometry. Accordingly, in our proposed model below, large-scale instabilities will be regarded as belonging to the spiral-mode family. (In a study on choked jet noise Westley & Woolley (1968) reported the observations of large-scale spiral-mode jet oscillations.)

A theoretical investigation of large-scale spiral-mode instability of a supersonic jet reveals that a spectrum of such unstable waves exist (some pertinent mathematical details will be given in § 4). Shadowgraphic observations, however, seem to indicate that not all these waves are excited. In § 5 it will be shown that in a supersonic jet there is a natural selection mechanism which tends to amplify only two of all these waves. This selection mechanism is provided by the large-scale periodic flow structure of the jet immediately downstream of the nozzle exit.

It is known (see Pack 1950; Love *et al.* 1959) that downstream of the nozzle exit of a nearly ideally expanded supersonic jet, the jet flow develops into a series

of almost periodic cell-like structures. The wave-number k_0 of these cells is approximately given by the following formula first derived by Prandtl (1904)

$$k_0 = 2\beta_1/D(M_j^2-1)^{\frac{1}{2}},$$

where β_1 is the first zero of the zeroth-order Bessel function ($\beta_1 = 2{\cdot}40483$); D is the diameter of the ideally expanded jet and M_j is the Mach number of the jet. As the fluid of the jet emerges from the nozzle it inevitably carries with it disturbances of various wavelengths. When these disturbances are convected through the periodic flow structure of the jet two waves will experience periodic resonant excitation (a mathematical description of this process will be given in §5). If k_1 and k_2 are the wave-numbers of these two waves, they are identified by the property that $k_1 - k_2 = k_0$. Physically, this periodic resonant excitation process is analogous to the transverse oscillation of an elastic string excited by periodic axial displacement of one of its ends (see Carrier 1970). Mathematically, it is analogous to a dynamical system described by the Mathieu equation. These two excited waves grow in amplitude on propagating downstream and eventually cause large-scale spiral-mode instabilities of the jet with the axial wave-numbers of the spiral-mode unstable waves equal to k_1 and k_2. That is to say, the axial wavelengths of the spiral-mode unstable waves are the same as those of the two waves excited by periodic resonance.

Of the two selectively excited spiral-mode unstable waves the one having a larger wave-number, k_1, has a shorter wavelength and a higher frequency. Also as will be shown in §4 it has a higher spatial growth rate than the other (long) wave. Thus the amplitude of this high frequency unstable wave will grow much faster than that of the low frequency wave. As a result, it will interact strongly with the ambient fluid on penetrating the mixing layer surrounding the jet at a location much closer to the nozzle exit than the lower frequency wave would. Being a short wave it involves only a very small fraction of the kinetic energy of the jet (mainly that of the fluid on the outer part of the jet) and hence its interaction with ambient fluid is relatively mild. The result of the interaction is a rapid disintegration of the unstable wave coupled with a thickening of the mixing layer and the emission of noise with a predominant frequency equal to the oscillation frequency of the unstable wave. In this way the high frequency unstable wave is responsible for the formation of a strong but localized noise source in the supersonic jet. Downstream from this high frequency noise source only the long wave remains. The oscillatory motion of the jet associated with this wave is shielded from the ambient fluid by the mixing layer, now thickened by the disintegration of the high frequency wave. Farther downstream the rapid growth in amplitude of the unstable long wave will finally allow it to penetrate the mixing layer and interact strongly with the ambient fluid to form a powerful low frequency noise source. As a good fraction of the jet energy is involved in this wave its destruction after interacting with the ambient fluid marks the beginning of the disintegration of the jet as an organized entity.

The above physical process explains the formation of two strong but localized noise sources in a nearly ideally expanded supersonic jet. It also implies that the frequencies corresponding to the peak and bulge (possibly a local peak) of the

jet noise power spectrum (figure 9) are equal to the frequencies of the spiral-mode unstable waves. Thus these frequencies can be predicted with good accuracy from first principles by hydrodynamic stability theory. Explicit expressions so obtained will be given in §6. They will be used for comparison with experimental measurements in §7.

Now let us estimate the approximate positions of the two strong noise sources within the framework of the model described above. In order that the selective excitation mechanism of our model can be effective, the initial disturbances from the nozzle must travel at least, say, a distance of 3 cell lengths inside the jet. Too short a distance will not allow enough time for resonant amplification to take place. The subsequent development of spiral-mode instability into large amplitude oscillations requires a distance of, say, 2 or 3 wavelengths. This depends, of course, on the spatial growth rate of each wave which in turn depends on the Mach number of the jet (growth rate decreases with increase in Mach number). Therefore if L_1 and L_2 denote the locations of the high and low frequency noise sources measured from the nozzle exit, then we expect

$$\left.\begin{aligned} L_1 &\simeq 3\lambda_0 + 2\lambda_1, \\ L_2 &\simeq 3\lambda_0 + (2 \text{ or } 3)\lambda_2, \end{aligned}\right\} \tag{1}$$

where $\lambda_0 = 2\pi/k_0$ is the wavelength of cells, $\lambda_1 = 2\pi/k_1$ is the wavelength of the high frequency unstable wave and $\lambda_2 = 2\pi/k_2$ is the wavelength of the low frequency unstable wave. In (1) we note that the long wave has a smaller spatial growth rate than the short wave. Hence a slightly larger coefficient in front of λ_2 than λ_1 would be appropriate. Expression (1) will be used for qualitative comparison with experimental values in §7.

Now let us turn to the generation mechanisms of the very high and very low frequency noise shown in the power spectrum of figure 9. They correspond to frequencies to the right of the bulge and to the left of the peak in this figure. So far we have ignored the non-linearities of the fluid flow. We believe that the very high frequency noise is emitted principally by small amplitude higher order waves created through non-linearities in the presence of spiral mode instabilities. The very low frequency noise is known to be generated downstream of the localized low frequency noise source. We note that in this region the long spiral-mode unstable wave decays at an appreciable rate after interacting strongly with the ambient fluid earlier upstream. During this decaying process the rate of oscillation is gradually being slowed down owing to the intense mixing of the jet and ambient fluids. At the same time the organized spiral-mode structure disappears slowly over a distance of a few wavelengths (see figure 10). Some residue kinetic energy is still contained in the slowed-down spiral oscillations. The continuous interaction of these slowed-down oscillations with surrounding fluid is responsible for the generation of lower and lower frequency noise at a much reduced intensity.

A mathematical analysis of the large-scale jet instability model described above will be presented in the next three sections of this paper. In §3 the periodic flow structure of a nearly ideally expanded supersonic jet will be briefly examined. Section 4 is devoted to a study of large-scale spiral-mode jet instability with

spatial growth rate. In § 5, the resonant instability mechanism by which waves of wave-numbers k_1 and k_2 are selected will be described.

3. The flow structure of a nearly ideally expanded supersonic jet

In this section we want to investigate the flow structure of a nearly ideally expanded supersonic jet. We will show in later sections that this structure plays a crucial role in the selective amplification of unstable waves and in the determination of the frequency corresponding to the peak of the power spectrum of the noise of such a jet. The present problem is not new. It has been discussed theoretically by Prandtl (1904), Pack (1950) and experimentally by Love *et al.* (1959). Here we will not dwell on the problem in any great length but briefly summarize the results that are pertinent to the development of this paper.

Of all the dynamical effects that are relevant in determining the flow structure of a supersonic jet, inertia and compressibility are the most important. Viscous forces are relatively unimportant except in the thin mixing layer at the outer edge of the jet. Close to the nozzle exit a good first approximation is to assume that the jet fluid is inviscid and the mixing layer is infinitesimally thin. Let p_a be the pressure of the stationary ambient fluid and $p_1 + \Delta p$ be the static pressure of the supersonic jet at the nozzle exit. If Δp is zero, within the model adopted, a uniform jet with velocity parallel to the jet axis will be formed. If Δp is small but not zero we expect the jet to remain nearly uniform save for some small perturbations of the order of Δp. To find these perturbations to order Δp a linear analysis is adequate.

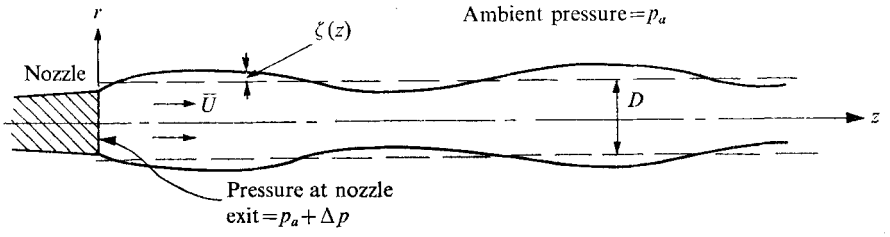

FIGURE 12. Structure of a nearly ideally expanded inviscid supersonic jet.

Let D be the diameter of the jet and $\bar{U}$ be the jet velocity if the jet were ideally expanded to ambient pressure p_a as shown in figure 12. (D is not equal to the exit diameter of the nozzle unless Δp is zero.) Inside the jet the perturbation equations are

$$\bar{\rho}_j \nabla . \mathbf{v} + \bar{U}\, \partial \rho / \partial z = 0, \tag{2}$$

$$\bar{\rho}_j \bar{U}\, \partial \mathbf{v} / \partial z = -\nabla p, \tag{3}$$

$$p = a_j^2 \rho. \tag{4}$$

These are the linearized continuity, momentum and energy equations. Here $\bar{\rho}_j$ and a_j denote the mean density and sound speed of the ideally expanded jet and $\mathbf{v}, p$ and ρ denote the perturbation velocity, pressure and density respectively. By eliminating $\mathbf{v}$ and ρ, the pressure perturbation is found to be given by

$$\frac{\partial^2 p}{\partial r^2} + \frac{1}{r}\frac{\partial p}{\partial r} - (M_j^2 - 1)\frac{\partial^2 p}{\partial z^2} = 0, \tag{5}$$

where $M_j = \bar{U}/a_j$ is the Mach number of the ideally expanded jet. The boundary conditions are

$$r = \tfrac{1}{2}D \quad \text{when} \quad p = 0, \tag{6}$$

$$-\frac{1}{\bar{\rho}_j}\frac{\partial p}{\partial r} = \bar{U}^2\frac{\partial^2\zeta}{\partial z^2}, \tag{7}$$

$$\left.\begin{aligned} p &= \Delta p, \\ \mathbf{v} &\text{ is parallel to the jet axis,} \end{aligned}\right\} \quad \text{at} \quad z = 0 \tag{8, 9}$$

where $\zeta(z)$ is the radial displacement of the jet boundary as shown in figure 12. Conditions (6) and (7) are the dynamic and kinematic boundary conditions respectively and (8) and (9) are boundary conditions at the nozzle exit which are responsible for causing the perturbations in the jet flow. Condition (9) is, of course, not in its most general form. The present form is used solely to simplify the calculation and is not significant in influencing the final results of this paper.

An appropriate solution to the above equations and boundary conditions is

$$\left.\begin{aligned} p &= \sum_{\mu=1}^{\infty} A_\mu J_0\left(\frac{2r\beta_\mu}{D}\right)\cos\left(\frac{2\beta_\mu z}{D(M_j^2-1)^{\frac{1}{2}}}\right), \\ v_z &= -\frac{1}{\bar{\rho}_j\bar{U}}\sum_{\mu=1}^{\infty} A_\mu J_0\left(\frac{2r\beta_\mu}{D}\right)\cos\left(\frac{2\beta_\mu z}{D(M_j^2-1)^{\frac{1}{2}}}\right), \\ v_r &= \frac{(M_j^2-1)^{\frac{1}{2}}}{\bar{\rho}_j\bar{U}}\sum_{\mu=1}^{\infty} A_\mu J_1\left(\frac{2r\beta_\mu}{D}\right)\sin\left(\frac{2\beta_\mu z}{D(M_j^2-1)^{\frac{1}{2}}}\right), \\ \zeta &= -\frac{(M_j^2-1)D}{2\bar{\rho}_j\bar{U}^2}\sum_{\mu=1}^{\infty}\frac{A_\mu}{\beta_\mu}J_1(\beta_\mu)\cos\left(\frac{2\beta_\mu z}{D(M_j^2-1)^{\frac{1}{2}}}\right) + \text{constant}, \\ \rho &= p/a_j^2, \quad A_\mu = 2\Delta p/\beta_\mu J_1(\beta_\mu), \end{aligned}\right\} \tag{10}$$

where J_0 and J_1 are the Bessel functions of order zero and one respectively and β_μ denotes the μth root of $J_0(\beta_\mu) = 0$.

From (10) it is clear that close to the nozzle exit an almost periodic flow structure exists. To a good approximation the wavelength of this structure is given by that of the first term of the series in (10) (see Prandtl). That is to say, the wavelength $\sim \pi(M_j^2-1)^{\frac{1}{2}}D/\beta_1$ ($\beta_1 = 2{\cdot}40483$). Of course viscosity and the mixing process will ultimately destroy this periodic structure but this will take place many jet diameters downstream.

4. Large-scale spiral-mode instability characteristics of a cold supersonic jet

In this section the spiral-mode spatial instability characteristics of a supersonic jet will be studied. In the past, theoretical investigations on the stability of an inviscid compressible jet have been carried out by many authors, for example, Lessen *et al.* (1965), Gill & Drazin (1965). However, their works are all confined to unstable waves with temporal growth rates. The physical problem that we are presently investigating involves unstable waves which grow spatially rather than temporally. Spatial instability characteristics (frequency and wave-number

relationships) of a supersonic jet do not seem to be readily available in the literature. The prime purpose of this present brief investigation is to obtain vital numerical information that is pertinent to the supersonic jet noise problem.

In a supersonic jet the velocity inside the supersonic core is very high. Surrounding the core is a mixing layer in which the fluid velocity decreases radially until a negligible value is reached at its outer edge. The mixing layer at a distance not too far downstream of the nozzle exit is relatively thin and dynamically unimportant as far as large-scale instability is concerned. In this section we will adopt a simple model in which the thickness of the mixing layer is essentially zero† on comparison with the diameter of the jet and the wavelengths of the unstable waves. The velocity profile inside a real jet is to a large extent unknown, even experimentally. A reasonably good approximation for our present purpose, perhaps, is to consider the velocity there to be constant. In the following we will use the model of an uniform jet bounded by a vortex sheet as shown in figure 13 with the understanding that it is only a first approximation to a real supersonic jet.

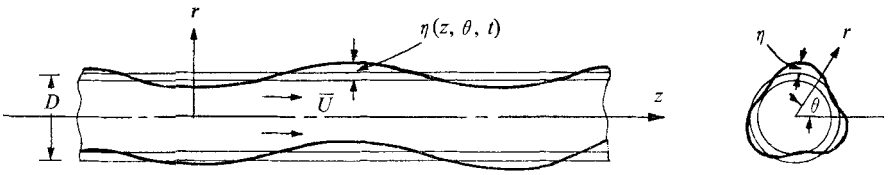

FIGURE 13. Instability of a supersonic jet bounded by a vortex sheet.

Let us denote the pressure perturbations, the unperturbed densities, the sound speeds, the velocity and diameter of the jet by p_o, p_j, $\bar{\rho}_o$, $\bar{\rho}_j$, a_o, a_j, $\bar{U}$ and D respectively with subscripts o and j indicating variables outside and inside the jet. From the linearized equations of motion the pressure perturbations are found to be governed by the following convected wave equations.

$$\partial^2 p_o/\partial t^2 = a_o^2 \nabla p_o, \quad r > \tfrac{1}{2}D, \tag{11}$$

$$\left(\frac{\partial}{\partial t} + \bar{U}\frac{\partial}{\partial z}\right)^2 p_j = a_j^2 \nabla^2 p_j, \quad r < \tfrac{1}{2}D. \tag{12}$$

If $\eta(z, \theta, t)$ represents the radial displacement of the vortex sheet at the outer boundary of the jet as shown in figure 13, then the kinematic and dynamic boundary conditions at the vortex sheet are

$$\left.\begin{aligned} -\frac{1}{\bar{\rho}_o}\frac{\partial p_o}{\partial r} = \frac{\partial^2 \eta}{\partial t^2}, \quad -\frac{1}{\bar{\rho}_j}\frac{\partial p_j}{\partial r} = \left(\frac{\partial}{\partial t} + \bar{U}\frac{\partial}{\partial z}\right)^2 \eta \\ p_o = p_j \end{aligned}\right\} \quad \text{for} \quad r = \tfrac{1}{2}D. \tag{13}$$

In addition, the finiteness condition requires that

$$\left.\begin{aligned} &p_j \text{ remains finite} \quad \text{as} \quad r \to 0, \\ &p_o \to 0 \text{ for finite } t \quad \text{as} \quad r \to \infty. \end{aligned}\right\} \tag{14}$$

† Dynamically it is the momentum thickness of the mixing layer which is important. Based on the limited data of Eggers (1966) on a 2·22 Mach number jet this is estimated to be a reasonable approximation.

On considering solutions of (11) to (14) of the form $p \sim f(r)e^{i(kz+m\theta-\omega t)}$ with $m = 1$ (spiral mode) it is straightforward to deduce that the wave-number k and frequency ω are related by the following eigenvalue equation.

$$\Omega^2\xi_j \frac{dJ_1(\xi_j)}{d\xi_j} H_1^{(1)}(\xi_o) - \left(\frac{a_o}{a_j}\right)^2 \left(\Omega - \frac{\overline{U}}{a_o}\kappa\right)^2 \xi_o \frac{dH_1^{(1)}(\xi_o)}{d\xi_o} J_1(\xi_j) = 0, \tag{15}$$

where

$$\xi_o = (\Omega^2 - \kappa^2)^{\frac{1}{2}},$$

$$\xi_j = \left[\left(\frac{a_o}{a_j}\right)^2 \left(\Omega - \frac{\overline{U}}{a_o}\kappa\right)^2 - \kappa^2\right]^{\frac{1}{2}},$$

$$\Omega = \omega D/2a_o, \quad \kappa = \tfrac{1}{2}kD,$$

and $J_1(\xi)$ is the Bessel function of order 1, $H_1^{(1)}(\xi)$ is the Hankel function of the first kind of order 1. The branch cuts for ξ_o and ξ_j are taken to be such that $\mathrm{Im}\,(\xi_o)$, $\mathrm{Im}\,(\xi_j) > 0$. (In deriving (15) the specific heat ratios of the jet and ambient fluids are considered to be equal.)

In the present problem we are interested primarily in spatially growing instabilities. In recent years the theory of spatially growing unstable waves has been elaborated by Briggs (1964), Gaster (1963, 1965), Michalke (1965) and others. For the present purpose an investigation following Briggs shows that the instabilities are convective in the direction of the jet flow and it is sufficient to look for eigenvalues of (15) with ω real and k complex ($k = k_r + ik_i$) for spatially growing waves. Unstable waves propagating in the downstream direction are given by eigenvalues with $k_i < 0$.

In (15) there are two independent physical parameters, namely, a_o/a_j and $\overline{U}/a_o$. For a cold jet in which the total temperatures of the jet and ambient fluid are the same these two parameters are related and the problem has only one free parameter. The eigenvalues of (15) corresponding to a cold supersonic jet with the Mach number of the jet $M_j = \overline{U}/a_j$, chosen as the independent parameter have been obtained numerically using the facilities of the M.I.T. Computer Centre. Figure 14 shows a sample of the relationships between k_r and ω for various values of $1{\cdot}5 \leqslant M_j \leqslant 4{\cdot}0$. Figure 15 gives the relationships between $-k_i$ and ω for the same range of Mach numbers. A study of figure 14 reveals that for a fixed jet Mach number M_j, k_r and ω are almost a linear function of each other. On using a straight line approximation (dotted lines in figure 14) it is possible to express the dependence of ω on k_r in a simple analytical form. A good fit is found numerically to be

$$\left.\begin{aligned}\tfrac{1}{2}k_r D = [1{\cdot}046 - 0{\cdot}198(M_j - 1{\cdot}40627)^{\frac{1}{2}}]\,[\omega D/2a_o + 0{\cdot}033M_j^2 - 0{\cdot}219M_j + 0{\cdot}207]\\ \text{(cold jet, } 1{\cdot}5 \leqslant M_j \leqslant 4{\cdot}0\text{, spiral mode).}\end{aligned}\right\} \tag{16}$$

Instead of choosing M_j to be the independent parameter the ratio $\overline{U}/a_o$ can also be used. In terms of $\overline{U}/a_o$ a good approximate relation between k_r and ω can be found in a similar manner:

$$\left.\begin{aligned}\tfrac{1}{2}k_r D = [1{\cdot}436 - 0{\cdot}361\,\overline{U}/a_o]\,\{\omega D/2a_o - 0{\cdot}198 + [0{\cdot}00126 + 0{\cdot}044(\overline{U}/a_0 - 1{\cdot}915)^2]^{\frac{1}{2}}\}\\ \text{(cold jet, } 1{\cdot}246 \leqslant \overline{U}/a_o \leqslant 1{\cdot}952\text{, spiral mode).}\end{aligned}\right\} \tag{17}$$

By means of (16) and (17) the frequency of large-scale spiral-mode oscillation can be determined once the wavelength or wave-number of an unstable wave is selected. Figure 15 shows that as M_j increases the spatial growth rate of unstable waves decreases. That is to say, for a high Mach number jet it is necessary for an unstable wave to propagate over a longer distance before it can acquire a sufficiently large amplitude.

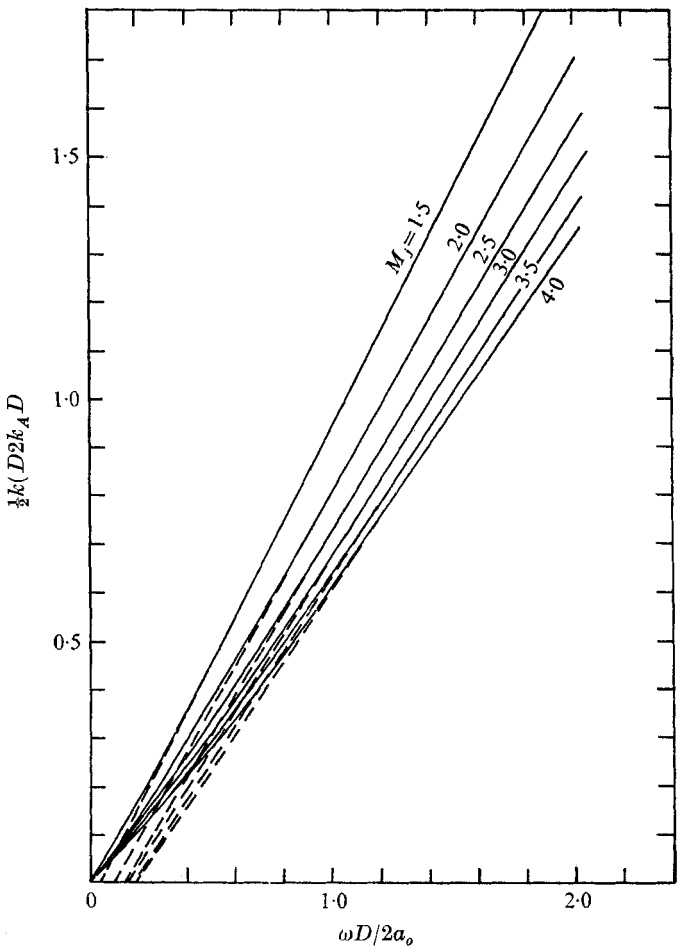

FIGURE 14. Instability characteristics of a cold supersonic jet bounded by a vortex sheet (spiral mode). —, exact; – – –, approximation by straight lines; $M_j = \bar{U}/a_j$ = Mach number of supersonic jet.

5. Resonant excitation mechanism

Now a mechanism by which two large-scale unstable waves are preferentially selected in a nearly ideally expanded supersonic jet as mentioned in §2 will be discussed. Inside the nozzle of the jet disturbances are continuously being generated. These disturbances are then convected downstream by the supersonic

flow. On emerging from the nozzle exit they pass through the large-scale periodic structure of the jet discussed in §3. In so doing the disturbances experience periodic excitation. We will show below that for disturbances of certain wavelengths this periodic excitation immediately leads to resonance and hence exponential growth.

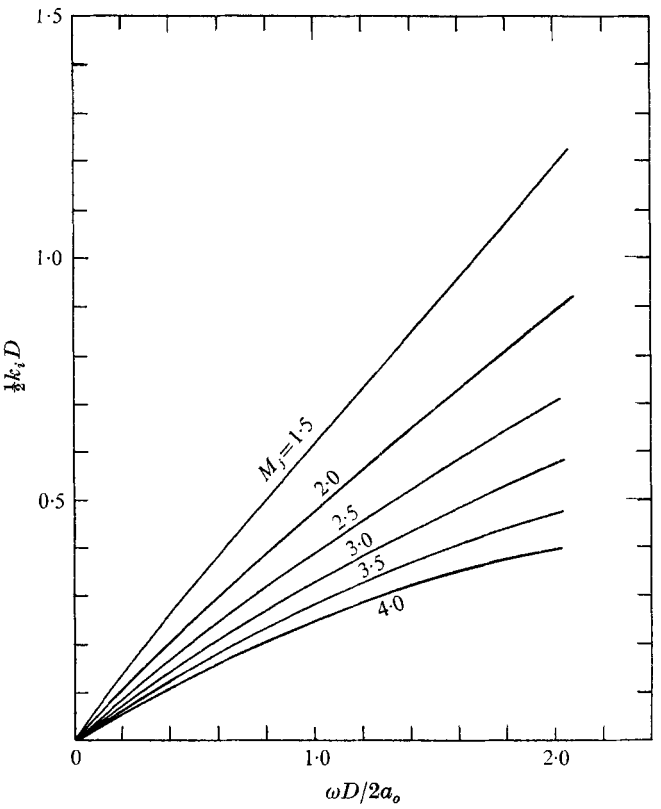

FIGURE 15. Instability characteristics of a cold supersonic jet bounded by a vortex sheet (spiral mode).

Near the nozzle exit all the disturbances generated upstream are confined within the jet. The fluid velocity is supersonic in this region and flows mainly in the downstream direction. As a result, disturbances propagate essentially only in the axial direction of the jet. That is, to a good approximation radial spreading of the disturbances can be neglected at least within a short distance of say 3 cell lengths measured from the nozzle exit. With this in mind, in the following we will adopt a one-dimensional mathematical model in which only the propagation of disturbances in the axial direction of the jet is considered so as to reduce mathematical complications. It is to be understood that farther downstream this one-dimensional model will no longer be valid and the unstable waves will become three-dimensional.

Let us now consider how disturbances will propagate near the nozzle exit.

The equations of continuity, momentum and energy governing the one-dimensional flow of a perfect gas are

$$\left.\begin{aligned} \frac{\partial \rho}{\partial t}+\frac{\partial(\rho u)}{\partial z}=0, \quad \rho\left(\frac{\partial u}{\partial t}+u\frac{\partial u}{\partial z}\right)=-\frac{\partial p}{\partial z}, \\ \frac{\partial p}{\partial t}+\frac{\partial(pu)}{\partial z}+(\gamma-1)p\frac{\partial u}{\partial z}=0, \end{aligned}\right\} \tag{18}$$

where u is the velocity in the z direction and γ is the specific heat ratio.

Near the axis of the supersonic jet the periodic component of the mean flow field is approximately given by the first term of (10). The mean flow field can be written as

$$\tilde{p}=\bar{p}_j+\epsilon\cos k_0 z, \quad \rho=\bar{\rho}_j+(\epsilon/a_j^2)\cos k_0 z, \quad \tilde{v}_z=\bar{U}-(\epsilon/\bar{\rho}_j\,\bar{U})\cos k_0 z, \quad \tilde{v}_r\simeq 0, \tag{19}$$

with $$k_0=2\beta_1/D(M_j^2-1)^{\frac{1}{2}}, \quad \epsilon=2\Delta p/\beta_1 J_1(\beta_1).$$

The equations governing the propagation of small disturbances with a mean flow given by (19) can be obtained by a straightforward linearization of (18). Since these disturbances are propagating waves they can be expressed mathematically in the following form.

$$p'=\hat{p}(z)e^{-i\omega t}, \quad \rho'=\hat{\rho}(z)e^{-i\omega t}, \quad u'=\hat{u}(z)e^{-i\omega t}. \tag{20}$$

The amplitude functions $\hat{p}(z)$, $\hat{\rho}(z)$, $\hat{u}(z)$ are to be determined from the linearized equations which are as follows.

$$\left.\begin{aligned} &-i\omega\hat{\rho}+\bar{\rho}_j\frac{d\hat{u}}{dz}+\bar{U}\frac{d\hat{\rho}}{dz}+\epsilon\left[\frac{1}{a_j^2}\frac{d\hat{u}}{dz}\cos k_0 z+\frac{k_0}{\bar{\rho}_j\,\bar{U}}\hat{\rho}\sin k_0 z\right.\\ &\qquad\left.-\frac{1}{\bar{\rho}_j\,\bar{U}}\frac{d\hat{\rho}}{dz}\cos k_0 z-\frac{k_0}{a_j^2}\hat{u}\sin k_0 z\right]=0,\\ &-i\omega\bar{\rho}_j\hat{u}+\bar{\rho}_j\,\bar{U}\frac{d\hat{u}}{dz}+\frac{d\hat{p}}{dz}+\epsilon\left[-\frac{i\omega}{a_j^2}\hat{u}\cos k_0 z+\frac{k_0}{\bar{U}}\hat{u}\sin k_0 z\right.\\ &\qquad\left.+\frac{k_0}{\bar{\rho}_j}\hat{\rho}\sin k_0 z+\left(\frac{\bar{U}}{a_j^2}-\frac{1}{\bar{U}}\right)\frac{d\hat{u}}{dz}\cos k_0 z\right]=0,\\ &-i\omega\hat{p}+\gamma\bar{p}_j\frac{d\hat{u}}{dz}+\bar{U}\frac{d\hat{p}}{dz}+\epsilon\left[\gamma\frac{d\hat{u}}{dz}\cos k_0 z+\frac{\gamma k_0}{\bar{\rho}_j\,\bar{U}}\hat{p}\sin k_0 z\right.\\ &\qquad\left.-k_0\hat{u}\sin k_0 z-\frac{1}{\bar{\rho}_j\,\bar{U}}\frac{d\hat{p}}{dz}\cos k_0 z\right]=0. \end{aligned}\right\} \tag{21}$$

The above system of equations (21), resembles very much the Mathieu equation. As is well known, the Mathieu equation possesses resonant unstable solutions. We therefore expect this system of equations also to possess resonant unstable solutions. The treatment of resonant instability of the Mathieu equation has been given by various authors in the past. Recently, Cole (1968) gave a particularly illuminating treatment of this phenomenon by a two-variable expansion procedure. Here we will follow this method of Cole. According to this method a

slow variable $\tilde{z} = \epsilon z$ is introduced and the functions $\hat{p}, \hat{\rho}$ and $\hat{u}$ are to be expanded in a power series of ϵ.

$$\left.\begin{aligned}\hat{p}(z,\tilde{z}) &= \hat{p}_0(z,\tilde{z}) + \epsilon\hat{p}_1(z,\tilde{z}) + \ldots,\\ \hat{\rho}(z,\tilde{z}) &= \hat{\rho}_0(z,\tilde{z}) + \epsilon\hat{\rho}_1(z,\tilde{z}) + \ldots,\\ \hat{u}(z,\tilde{z}) &= \hat{u}_0(z,\tilde{z}) + \epsilon\hat{u}_1(z,\tilde{z}) + \ldots.\end{aligned}\right\} \tag{22}$$

On substituting (22) into (21) and on partitioning terms according to powers of ϵ we have to zeroth order

$$\left.\begin{aligned}-i\omega\hat{\rho}_0 + \bar{\rho}_j\frac{\partial\hat{u}_0}{\partial z} + \overline{U}\frac{\partial\hat{\rho}_0}{\partial z} &= 0,\\ -i\omega\bar{\rho}_j\hat{u}_0 + \bar{\rho}_j\overline{U}\frac{\partial\hat{u}_0}{\partial z} + \frac{\partial\hat{p}_0}{\partial z} &= 0,\\ -i\omega\hat{p}_0 + \gamma\bar{p}_j\frac{\partial\hat{u}_0}{\partial z} + \overline{U}\frac{\partial\hat{p}_0}{\partial z} &= 0,\end{aligned}\right\} \tag{23}$$

and to order ϵ

$$-i\omega\hat{\rho}_1 + \bar{\rho}_j\frac{\partial\hat{u}_1}{\partial z} + \overline{U}\frac{\partial\hat{\rho}_1}{\partial z} = -\bar{\rho}_j\frac{\partial\hat{u}_0}{\partial\tilde{z}} - \overline{U}\frac{\partial\hat{\rho}_0}{\partial\tilde{z}} - \frac{1}{a_j^2}\frac{\partial\hat{u}_0}{\partial z}\cos k_0 z - \frac{k_0}{\bar{\rho}_j\overline{U}}\hat{\rho}_0\sin k_0 z$$
$$+\frac{1}{\bar{\rho}_j\overline{U}}\frac{\partial\hat{\rho}_0}{\partial z}\cos k_0 z + \frac{k_0}{a_j^2}\hat{u}_0\sin k_0 z, \tag{24}$$

$$-i\omega\bar{\rho}_j\hat{u}_1 + \bar{\rho}_j\overline{U}\frac{\partial\hat{u}_1}{\partial z} + \frac{\partial\hat{p}_1}{\partial z} = -\bar{\rho}_j\overline{U}\frac{\partial\hat{u}_0}{\partial\tilde{z}} - \frac{\partial\hat{p}_0}{\partial\tilde{z}} + \frac{i\omega}{a_j^2}\hat{u}_0\cos k_0 z - \frac{k_0}{\overline{U}}\hat{u}_0\sin k_0 z$$
$$-\frac{k_0}{\bar{\rho}_j}\hat{\rho}_0\sin k_0 z - \left(\frac{\overline{U}}{a_j^2} - \frac{1}{\overline{U}}\right)\frac{\partial\hat{u}_0}{\partial z}\cos k_0 z = I_1, \tag{25}$$

$$-i\omega\hat{p}_1 + \gamma\bar{p}_j\frac{\partial\hat{u}_1}{\partial z} + \overline{U}\frac{\partial\hat{p}_1}{\partial z} = -\gamma\bar{p}_j\frac{\partial\hat{u}_0}{\partial\tilde{z}} - \overline{U}\frac{\partial\hat{p}_0}{\partial\tilde{z}} - \gamma\frac{\partial\hat{u}_0}{\partial z}\cos k_0 z - \frac{\gamma k_0}{\bar{\rho}_j\overline{U}}\hat{p}_0\sin k_0 z$$
$$+k_0\hat{u}_0\sin k_0 z + \frac{1}{\bar{\rho}_j\overline{U}}\frac{\partial\hat{p}_0}{\partial z}\cos k_0 z = J_1. \tag{26}$$

Let us look for propagating wave solutions of the form $\sim e^{ikz}$ to the zeroth-order equations. A straightforward calculation gives

$$\left.\begin{aligned}\hat{p}_0 &= A(\tilde{z})\,e^{ik_1 z} + B(\tilde{z})\,e^{ik_2 z},\\ \hat{u}_0 &= -\frac{A(\tilde{z})}{\bar{\rho}_j a_j}e^{ik_1 z} + \frac{B(\tilde{z})}{\bar{\rho}_j a_j}e^{ik_2 z},\\ \hat{\rho}_0 &= \hat{p}_0/a_j^2,\end{aligned}\right\} \tag{27}$$

where the wave-numbers k_1 and k_2 are related to ω by

$$k_1 = \frac{\overline{U} + a_j}{\overline{U}^2 - a_j^2}\omega, \quad k_2 = \frac{\overline{U} - a_j}{\overline{U}^2 - a_j^2}\omega, \tag{28}$$

$A(\tilde{z})$ and $B(\tilde{z})$ are arbitrary functions of $\tilde{z}$.

In introducing a slow variable $\tilde{z}$ we have implicitly assumed that the solutions are bounded in the fast variable z. In order for this to be true the non-homogeneous

terms in (25) and (26) must satisfy certain orthogonality conditions. These conditions can readily be established by integration by parts. They are

$$\lim_{L\to\infty}\frac{1}{L}\int_0^L(-a_jI_1+J_1)\,e^{-ik_1z}\,dz=0, \tag{29}$$

$$\lim_{L\to\infty}\frac{1}{L}\int_0^L(a_jI_1+J_1)\,e^{-ik_2z}\,dz=0. \tag{30}$$

These two orthogonality conditions provide the necessary equations for the determination of $A(\tilde{z})$ and $B(\tilde{z})$. By means of these equations it can easily be shown that $A(\tilde{z})$ and $B(\tilde{z})$ are in general well behaved. The exceptional case is when resonance occurs. This takes place when the following relationship is fulfilled.

$$k_1-k_2=k_0. \tag{31}$$

That is, on using (28),

$$k_1=\tfrac{1}{2}k_0(M_j+1),\quad k_2=\tfrac{1}{2}k_0(M_j-1),\quad M_j=\bar{U}/a_j. \tag{32}$$

In the case of resonance the orthogonality conditions become

$$\left.\begin{aligned}(\bar{U}-a_j)\frac{dA}{d\tilde{z}}+\frac{ik_0(M_j+1)}{8\bar{\rho}_ja_jM_j}((\gamma+1)M_j-2\gamma+2)B=0,\\ -\frac{ik_0(M_j-1)}{8\bar{\rho}_ja_jM_j}((\gamma+1)M_j+2\gamma-2)A+2(\bar{U}+a_j)\frac{dB}{d\tilde{z}}=0.\end{aligned}\right\} \tag{33}$$

These equations have solutions of the form $A=\tilde{A}e^{\nu\tilde{z}}$, $B=\tilde{B}e^{\nu\tilde{z}}$ ($\tilde{A},\tilde{B}$ are constants) with ν given by

$$\nu=\pm(k_0/8\bar{\rho}_ja_j^2M_j)\,[(\gamma+1)M_j+2\gamma-2]^{\frac{1}{2}}\,[(\gamma+1)M_j-2\gamma+2]^{\frac{1}{2}}.$$

This means that the waves will undergo resonant instability.

To sum up, we see that because of the periodic structure of the jet flow two waves with wave-numbers

$$k_1=\frac{\beta_1}{D}\left(\frac{M_j+1}{M_j-1}\right)^{\frac{1}{2}},\quad k_2=\frac{\beta_1}{D}\left(\frac{M_j-1}{M_j+1}\right)^{\frac{1}{2}}\quad(\beta_1=2{\cdot}4048) \tag{34}$$

will be selectively amplified by resonant excitation. These are the waves which are responsible for triggering large-scale spiral-mode instabilities in a supersonic jet as proposed in our physical model in § 2.

6. The frequency corresponding to the peak value of the power spectrum of radiated noise

In the last section we have shown that because of the periodicity of the jet structure near the nozzle exit resonant excitation causes the growth of waves with wave-numbers $k_1=\frac{1}{2}k_0(M_j+1)$ and $k_2=\frac{1}{2}k_0(M_j-1)$. On propagating downstream over a distance of 3 or 4 jet cell lengths these amplified disturbances will become strong enough to excite large-scale spiral-mode jet instabilities with the same axial wavelengths. These large-scale spiral-mode instabilities when effectively developed will be capable of transferring a part of the kinetic energy

of the jet into noise radiation by causing the jet fluid to interact with the surrounding fluid. A wave with axial wave-number k_1 has a shorter wavelength and the higher spatial growth rate (figure 15) brings about noise radiation at a higher frequency closer to the nozzle exit than a wave with wave-number k_2. We expect the location of maximum noise radiation corresponding to this wave to be at ~ 3 jet cell lengths (so that resonant excitation can be effective) plus ~ 2 wavelengths downstream of the nozzle exit. This is the distance at which the large-scale jet instability will most probably be fully developed and dissipation due to mixing with ambient fluid is strong. A wave with axial wave-number k_2 has a longer wavelength and lower frequency. We also expect the location of maximum noise radiation corresponding to this wave to be at ~ 3 jet cell lengths plus ~ 2 wavelengths downstream of the nozzle exit. The short wave involves kinetic energy mainly on the outer part of the jet while in the oscillations of the long wave the whole supersonic jet participates. Therefore, when fully developed, the long-wave oscillations contain a substantial fraction of the kinetic energy of the jet whereas the short wave has only a minor fraction. As a result, the dominant noise source of a supersonic jet will radiate at a frequency corresponding to the frequency of oscillation of the long wave, i.e. this is the frequency of the peak of the power spectrum of radiated noise. At the same time the oscillations of the short wave will probably contribute to a local peak or a bulge (see figure 9) in the same power spectrum. With the above physical picture in mind, by equating the wave-number of spiral-mode instability to k_2 (from (34) and (16)) we arrive at the following formula for the frequency f of the peak of the power spectrum of a nearly ideally expanded cold supersonic jet with Mach number M_j.

$$\frac{\pi f D}{a_o} = 1{\cdot}202\left(\frac{M_j-1}{M_j+1}\right)^{\frac{1}{2}}[1{\cdot}406-0{\cdot}198(M_j-1{\cdot}40627)^{\frac{1}{2}}]^{-1} - (0{\cdot}033M_j^2-0{\cdot}219M_j+0{\cdot}207), \tag{35}$$

where D = diameter of jet, a_o = ambient speed of sound ($1{\cdot}5 \leqslant M_j \leqslant 4{\cdot}0$, cold jet). If (17) is used instead of (16) we have

$$\frac{\pi f D}{a_o} = 1{\cdot}202\left(\frac{M_j-1}{M_j+1}\right)^{\frac{1}{2}}\left[1{\cdot}436-0{\cdot}361\frac{\bar{U}}{a_o}\right]^{-1}+0{\cdot}198 - \left[0{\cdot}00126+0{\cdot}044\left(\frac{\bar{U}}{a_o}-1{\cdot}915\right)^2\right]^{\frac{1}{2}} \quad (1{\cdot}246 \leqslant \bar{U}/a_o \leqslant 1{\cdot}952). \tag{36}$$

Also from k_1 of (34) we expect a local peak or a bulge in the power spectrum at frequency $\bar{f}$ to be given by the following formula.

$$\frac{\pi \bar{f} D}{a_o} = 1{\cdot}202\left(\frac{M_j+1}{M_j-1}\right)^{\frac{1}{2}}[1{\cdot}406-0{\cdot}198(M_j-1{\cdot}40627)^{\frac{1}{2}}]^{-1} - (0{\cdot}033M_j^2-0{\cdot}219M_j+0{\cdot}207) \tag{37}$$

or

$$\frac{\pi \bar{f} D}{a_o} = 1{\cdot}202\left(\frac{M_j+1}{M_j-1}\right)^{\frac{1}{2}}\left[1{\cdot}436-0{\cdot}361\frac{\bar{U}}{a_o}\right]^{-1} + 0{\cdot}198-\left[0{\cdot}00126+0{\cdot}044\left(\frac{\bar{U}}{a_o}-1{\cdot}915\right)^2\right]^{\frac{1}{2}}. \tag{38}$$

In the next section we will compare the predictions of these equations with experiment.

7. Comparison with experiment

Based on idealized physical models of the flow field of a supersonic jet we have in the previous sections derived a few theoretical results which we would now like to compare with experimental data.

Wavelength of large-scale spiral-mode instability

Large-scale spiral-mode instability of a cold supersonic jet operating near shock-free condition can be seen in shadowgraphs provided by Potter (1968) and also in a preliminary report by Potter & Jones under the same title. The Mach number of the jet is 2·49. From (34) the axial wavelength of the long unstable wave is

$$\lambda_2 = \frac{2\pi}{k_2} = \frac{\pi}{1{\cdot}202}\left(\frac{M_j+1}{M_j-1}\right)^{\frac{1}{2}} D. \tag{39}$$

For $M_j = 2{\cdot}49$ this gives $\lambda_2 = 4{\cdot}0D$. From the shadowgraphs of Potter and also of Potter & Jones we estimate that the wavelength of the observed large-scale oscillations to be $\sim 4D$. Figure 10 is a shadowgraph of a cold supersonic jet of $M_j = 2{\cdot}53$ taken at the M.I.T. Gas Turbine Laboratory. The theoretical value of λ_2 from (39) is $3{\cdot}98D$. On this shadowgraph we have marked the peaks of the long unstable wave. It is clear that the peaks are not very sharp. Our best estimate gives a wavelength of $\sim 4D$ which is in good agreement with theory.

Frequency corresponding to the peak of the power spectrum of noise radiated

Power spectra of noise radiated from cold supersonic jets have been measured by Yu & Dosanjh (1971), Potter (1968) and Dosanjh & Yu (1968). In the works of Potter and Dosanjh & Yu only power spectra per $\frac{1}{3}$ octave bands are given. In order to compare with the present theory we have converted them to power spectra per unit cycle. Potter's data give only one peak in the power spectrum. We believe that his measurements are not fine enough to show the minor peak or bulge at a higher frequency. Also the dominant peak is rather flat and so in comparing with theory our best estimate from his data will be quoted. The work of Dosanjh & Yu shows two distinct peaks in the $\frac{1}{3}$ octave power spectrum. On coverting to power per cycle the minor peak is less prominent and the main peak rather flat. These should be taken into consideration when comparing with theoretical predictions.

(i) In the work of Yu & Dosanjh (1971) $M_j = 1{\cdot}5$, $D = 0{\cdot}408$ in., speed of sound in ambient air used in theory $a_0 = 1100$ ft/sec.

At the peak: f(theoretical, equation (35)) = 6·1 kHz; f(observed) $\sim$ 6 kHz.

At the bulge: f(theoretical, equation (37)) = 28·6 kHz; f(observed) $\sim$ 25–30 kHz. (see figure 8).

(ii) In the work of Potter (1968) $M_j = 2{\cdot}49$, $D = 1$ in., $a_0 = 1100$ ft/sec.

At the peak: f(theoretical) = 4·5 kHz; f(observed) $\sim$ 3·5–5 kHz.

(iii) In the work of Dosanjh & Yu (1968) (slightly underexpanded jet) $M_j = 2{\cdot}23$, D(nozzle exit) = 0·482 in., $a_0 = 1100$ ft/sec.

At the peak: f(theoretical) = 8·5 kHz; f(observed) $\sim$ 7–9 kHz.

At the bulge: f(theoretical) = 20·6 kHz; f(observed) $\sim$ 21–22 kHz.

The present investigation is not capable of providing a rigorous determination of the locations of the dominant localized noise sources. However, the physical arguments that led to (1) do not seem to be unreasonable. On using (1) to estimate qualitatively the locations of these noise sources it is found that they are quite consistent with the observations of Yu & Dosanjh (1971), Potter (1968) and Mull & Erickson (1957). Of course, to locate these sources experimentally is in itself a major task and has not been done with complete certainty. Nevertheless it is important to find that the proposed model is at least in general agreement with experiments.

Useful supersonic jet noise data available in the literature are few and fragmentary. The above are all that we managed to find. On comparing with theoretical values it can be seen that there is fair agreement in general. Of course much more experimental evidence is needed before the present proposed theory can be accepted in its entirety. However, the above does seem to lend confidence in the physical mechanism described in § 2.

8. A scaling formula

It is possible to obtain a scaling formula on the total noise radiated from a supersonic jet based on the present proposed mechanism of noise generation. We note from the experimental power spectra of supersonic jet noise that only frequencies in the proximity of the peak of a power spectrum contribute significantly to the total radiated power. At the same time we also note that according to the proposed mechanism noise radiated at these frequencies is due to the large-scale oscillatory motions of the jet fluid. As the fluid in the oscillatory jet core interacts strongly with the ambient fluid intense mixing of these fluids takes place. The mixed fluid is highly turbulent so the range of frequencies of noise radiated from this turbulent fluid is rather broad even though the primary energy of noise comes from a single mode of jet oscillation. From this consideration we see that the total power radiated must be proportional to the rate at which the kinetic energy of the jet is dissipated through the interaction of the oscillatory motion of the jet and the surrounding fluid. The kinetic energy per unit volume of jet fluid which is related to the large-scale oscillatory motion is $\frac{1}{2}\bar{\rho}_j \langle u^2 \rangle$, where $\langle u^2 \rangle$ is the averaged square of the disturbance velocity. Therefore, if W denotes the total noise power radiated then

$$W \propto \bar{\rho}_j \langle u^2 \rangle \, \bar{U} D^2.$$

At high velocity we expect $\langle u^2 \rangle$ to scale like $\bar{U}^2$. Hence we recover the $\bar{U}^3$ scaling formula, i.e.

$$W \propto \bar{\rho}_j \, \bar{U}^3 D^2. \tag{40}$$

9. Discussion

So far in our numerical computation in §§ 4 and 6 we have restricted ourselves to the case of a cold supersonic jet. Of course this was done out of convenience rather than necessity. There is no fundamental difference in the noise generation mechanism between a hot and a cold jet.

In order to see the significance of the jet temperature some numerical calculations for hot jets have been made. Figures 16 and 17 show the instability characteristics of a jet with $\overline{U}/a_0 = 1{\cdot}667$ and $1{\cdot}246$ respectively for various values of $a_0/a_j = (T_0/T_j)^{\frac{1}{2}}$. It is clear from the curves of these figures that the numerical relation of k_r and ω for hot jets does not differ significantly from that of the cold

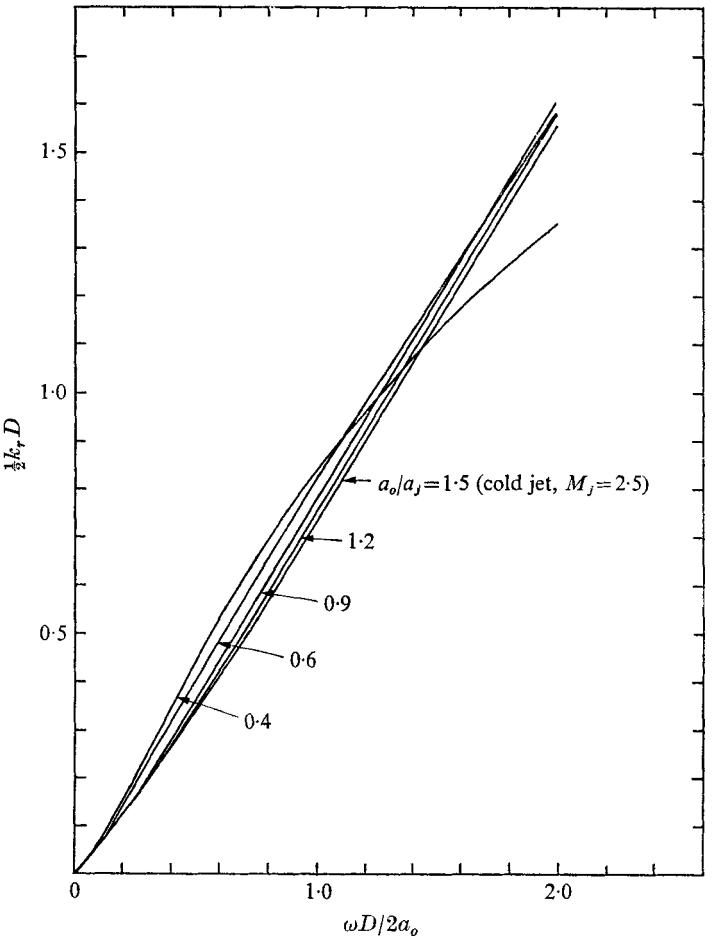

FIGURE 16. $\frac{1}{2}k_rD$ *vs.* $\omega D/2a_0$ at various jet temperatures. $U/a_0 = 1{\cdot}667$, spiral mode, a_0 = speed of sound in ambient gas, a_j = speed of sound inside jet.

jet over a wide range of temperature ratios. This means that if $\overline{U}/a_0$ is chosen as one of the two parameters of the problem the $k_r - \omega$ relation is not sensitive to changes in the other parameter involving the temperature of the jet. Equations (36) and (38) were derived from such a relation. Thus they can be used for hot as well as cold jets on allowing for a possible error of $\sim 10\ \%$. By means of these equations we see that for high Mach number jets, f(peak) is almost independent of temperature. This seems to indicate that the power spectrum would not be much affected by changes in the temperature of the jet.

In this paper we have examined the noise generation mechanism of nearly ideally expanded supersonic jets. For a moderately under-expanded or over-expanded jet certain modifications are necessary. First of all, the effective diameter of the jet will be quite different from the nozzle exit diameter. An estimate on the effective diameter of the jet based on mass continuity is required. Second,

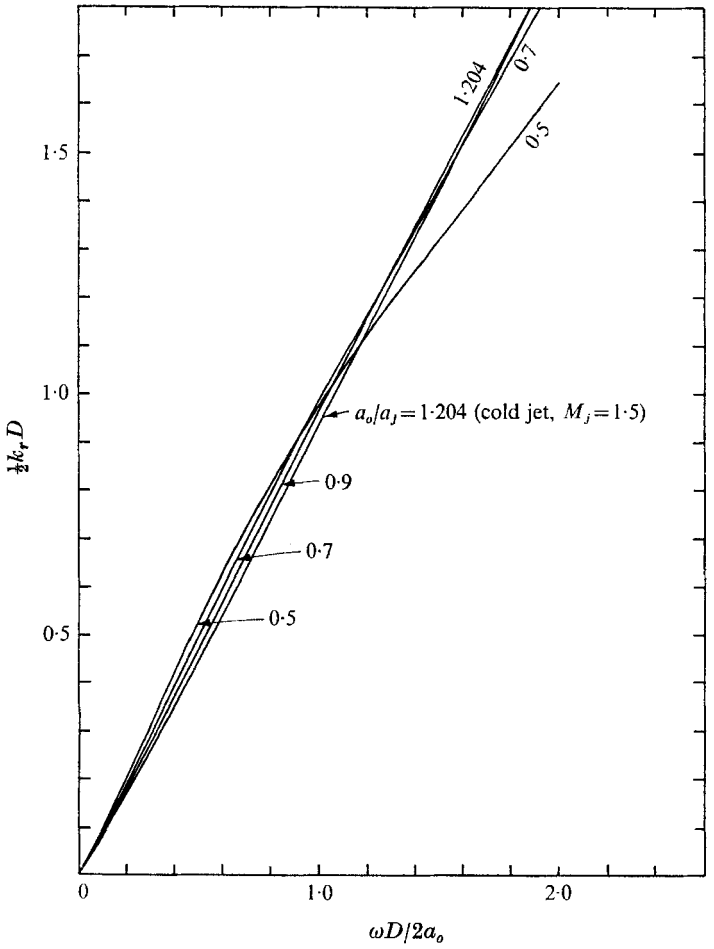

FIGURE 17. $\frac{1}{2}k_r D$ *vs.* $\omega D/2a_0$ at various jet temperatures. $U/a_o = 1{\cdot}246$, spiral mode.

shock cells will form in the jet flow and because of this, our estimates in § 3, which is based on linear analysis, will not be applicable without appropriate correction. Third, there is the possibility that the Mach number of the jet is not uniform even in the core of the jet owing to the presence of shocks. Thus a much better model of the velocity distribution across the jet is needed to estimate the instability characteristics of the jet flow. However, we believe that our proposed physical noise generation mechanism remains valid. This belief is supported by the experimental work of Yu & Dosanjh (1971).

In summary, we have proposed in the above a physical mechanism by which the dominant part of the noise of a nearly ideally expanded supersonic jet is generated. All the main features of this mechanism are found to be consistent with experimental observations. Theoretical predictions based on simple physical models of the jet flow according to the proposed mechanism compare favourably with the few shadowgraphic and far and near field noise measurements available in the literature. It is hoped that the present work provides certain insight into some physical aspects of supersonic jet noise.

REFERENCES

Berman, C. H. & Ffowcs Williams, J. E. 1970 Instability of two-dimensional compressible jet. *J. Fluid Mech.* **42**, 151.

Briggs, R. J. 1964 *Electron-stream Interaction with Plasmas*. M.I.T. Press.

Carrier, G. F. 1970 Stochastically driven dynamical systems. *J. Fluid Mech.* **44**, 249.

Cole, J. D. 1968 *Perturbation Methods in Applied Mathematics*. London: Blaisdell.

Crow, S. C. & Champagne, F. H. 1970 Orderly structure in jet turbulence. *Boeing Sci. Res. Lab. Document*, DI-82-0991.

Dosanjh, D. S. & Yu, J. C. 1968 Noise from underexpanded axisymmetric jet flow using radial jet flow impingement. *Proc. AFOSR-UTIAS Symp. on Aerodynamic Noise, Toronto*, 169–188.

Eggers, J. M. 1966 Velocity profiles and eddy viscosity distributions downstream of a Mach 2·2 nozzle exhausting to quiescent air. *N.A.S.A. Tech. Note*, D-3601.

Ffowcs Williams, J. E. 1963 The noise from turbulence convected at high speed. *Phil. Trans. Roy. Soc.* A**255**, 469.

Gaster, M. 1963 A note on a relation between temporally increasing and spatially increasing disturbances in hydrodynamic instability. *J. Fluid Mech.* **14**, 222.

Gaster, M. 1965 The role of spatially growing waves in the theory of hydrodynamic stability. *Prog. Aero. Sci.* **6**, 251.

Gill, A. E. & Drazin, P. G. 1965 Note on instability of compressible jets and wakes to long-wave disturbances. *J. Fluid Mech.* **22**, 415.

Jones, I. S. F. 1971 Finite amplitude waves from a supersonic jet. *A.I.A.A. Paper*, no. 71–151.

Lessen, M., Fox, J. A. & Zien, H. M. 1965 The instability of inviscid jets and wakes in compressible fluid. *J. Fluid Mech.* **21**, 129.

Lighthill, M. J. 1952 On sound generated aerodynamically I. General theory. *Proc. Roy. Soc.* A**211**, 564.

Lighthill, M. J. 1954 On sound generated aerodynamically II. Turbulence as a source of sound. *Proc. Roy. Soc.* A**222**, 1.

Lighthill, M. J. 1963 Jet noise (Wright Brothers Lecture). *A.I.A.A. J.* **1**, 1507.

Love, E. S., Grigsby, C. E., Lee, L. P. & Woodling, M. J. 1959 Experimental and theoretical studies of axisymmetric free jets. *N.A.S.A. Tech. Rep.* R-6.

Lowson, M. V. & Ollerhead, J. B. 1968 Visualization of noise from cold supersonic jets. *J. Acoust. Soc. Am.* **44**, 624.

Mayes, W. H., Lanford, W. E. & Hubbard, H. H. 1959 Near-field and far-field noise surveys of solid-fuel rocket engines for a range of nozzle exit pressures. *N.A.S.A. Tech. Note*, D-21.

Michalke, A. 1965 On spatially growing disturbances in an inviscid shear layer. *J. Fluid Mech.* **23**, 521.

Mull, H. R. & Erickson, J. C. 1957 Survey of the acoustic near field of three nozzles at a pressure ratio of 30. *N.A.C.A. Tech. Note*, 3978.

OLLERHEAD, J. B. 1966 Some shadowgraph experiments with a cold supersonic jet. *Wyle Lab. Res. Rep.* WR 66-44.

OLLERHEAD, J. B. 1967 On the prediction of the near field noise of supersonic jets. *N.A.S.A.*, CR-857.

PACK, D. C. 1950 A note on Prandtl's formula for the wavelength of a supersonic gas jet. *Quart. J. Mech. Appl. Math.* **3**, 173.

PHILLIPS, O. M. 1960 On the generation of sound by supersonic turbulent shear layers. *J. Fluid Mech.* **9**, 1.

POTTER, R. C. 1968 An investigation to locate the acoustic sources in a high speed jet exhaust stream. *Wyle Lab. Tech. Rep.* WR 68-4.

PRANDTL, L. 1904 *Phys. Zeits.* **5**, 599.

RIBNER, H. S. 1964 The generation of sound by turbulent jets. In *Advances in Applied Mechanics*, vol. 8, pp. 103–182. *Academic.*

RIBNER, H. S. 1969 Eddy Mach wave noise from a simplified model of a supersonic mixing layer. In *Basic Aerodynamic Noise Research.* N.A.S.A. SP-207.

TAM, C. K. W. 1971 Direction acoustic radiation from a supersonic jet generated by shear layer instability. *J. Fluid Mech.* **46**, 757.

WESTLEY, R. & WOOLLEY, J. H. 1968 An investigation of the near noise fields of a choked axisymmetric air jet. *Proc. AFOSR-UTIAS Symp. on Aerodynamic Noise, Toronto.*

YU, J. C. & DOSANJH, D. S. 1971 Noise field of coaxial interacting supersonic jet flows. *A.I.A.A. Paper*, no. 71–152.

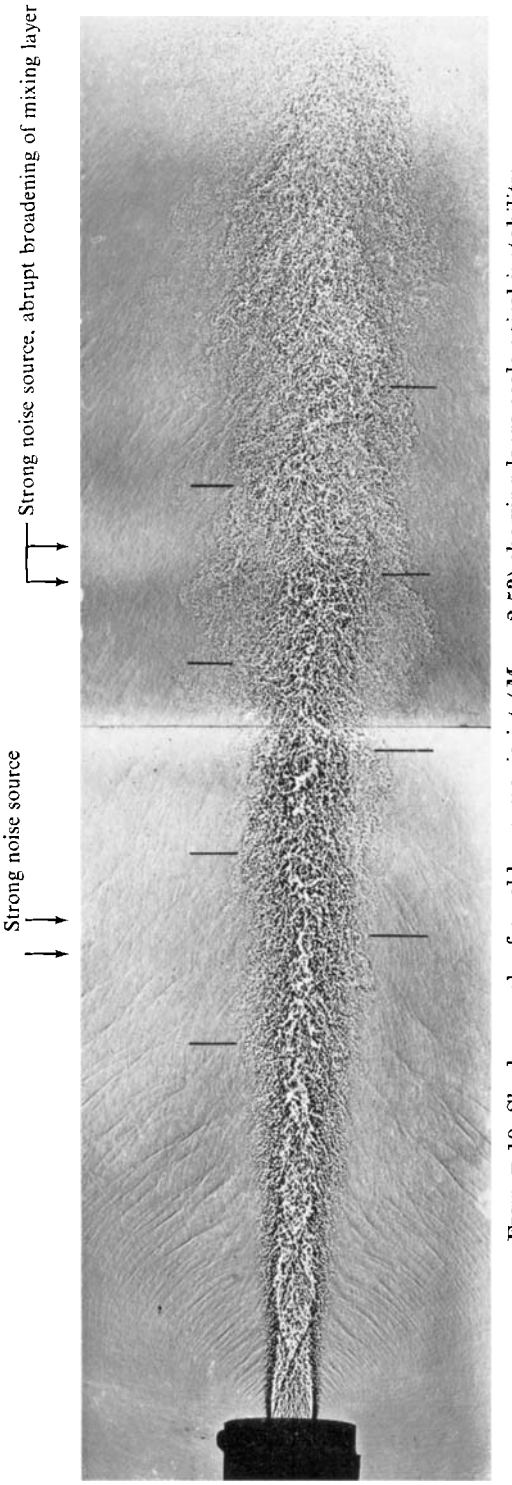

FIGURE 10. Shadowgraph of a cold supersonic jet ($M_j = 2{\cdot}53$) showing large-scale spiral instability.